sustainability

MDPI

Article

Risk Assessment and Spatial Distribution of Heavy Metals with an Emphasis on Antimony (Sb) in Urban Soil in Bojnourd, Iran

Abdulmannan Rouhani [1,*], Mohsen Makki [2], Michal Hejcman [1], Razieh Shirzad [3] and Mariusz Z. Gusiatin [4]

[1] Department of Environment, Faculty of Environment, The University of Jan Evangelista in Ústí nad Labem (UJEP), Pasteurova 1, 400 96 Ústí nad Labem, Czech Republic
[2] Geography Department, Humboldt-Universität zu Berlin, Unter den Linden 6, 10099 Berlin, Germany
[3] Department of Forestry, Faculty of Natural Resources, University of Tehran, Tehran 77871-31587, Iran
[4] Department of Environmental Biotechnology, Faculty of Geoengineering, University of Warmia and Mazury in Olsztyn, 10-720 Olsztyn, Poland
* Correspondence: a.rohani70@gmail.com

Abstract: Recently, one of the major environmental issues is the pollution of soil with Antimony (Sb), which is ecologically detrimental and potentially carcinogenic to humans. In developing countries such as Iran, Sb concentrations in soils have not yet been accurately determined. Therefore, the purpose of this study was to examine the levels of Sb and the other HMs (Pb, Cd, As, Ni, Hg and Cr) in the surface soils of Bojnourd, Iran, as well as their distribution and potential risks to the environment and human health. A total of 37 soil samples (0–20 cm) were taken from different sampling stations: 900 × 900 m regular grid for traffic areas (TA), residential areas (RA) and suburb areas (SA). The contamination factor (CF) and geo-accumulation index (I_{geo}) are two indices that were used to reflect the potential ecological risk from HMs. Geographic information system (GIS), Spearman correlation matrix and health risk indexes were utilized to investigate the source and potential hazard of HMs. The results showed that the average concentration of HMs in TA was highly enriched compared to other areas. Most soil samples were identified to have low levels of Sb and Ni pollution, while having moderate to high levels of Pb, Cr, As, Hg and Cd pollution, as determined by the pollution indices (I_{geo} and CF). Geostatistical analysis and GIS mapping of the spatial distribution of HM concentrations showed that there have been similar patterns of spatial distribution for Cd, Cr, Ni and Sb and their hot spots were in the southeast, west and center of the city. Neither the hazard quotient (HQ) nor the hazard index (HI) of the examined HMs indicated any non-carcinogenic risk to adults or children. However, carcinogenic risk assessment revealed that cancer risk was raised from Cr and Cd contents for children, while these elements showed an acceptable risk for adults. Furthermore, children's carcinogenic and non-carcinogenic values were greater than adults', indicating more potential health hazards associated with these HMs. Therefore, assessing the risk posed by HM pollution in urban surface soil is vital and urgent for children. A more detailed investigation is also required to identify the spatial distribution of soil pollution in areas recognized as enriched in Sb. A proper assessment of the environmental risk and the corresponding risk to humans from HM in a study area can be critical to developing an appropriate remediation method.

Keywords: urban soils; Antimony; heavy metals; pollution index; spatial distribution

Citation: Rouhani, A.; Makki, M.; Hejcman, M.; Shirzad, R.; Gusiatin, M.Z. Risk Assessment and Spatial Distribution of Heavy Metals with an Emphasis on Antimony (Sb) in Urban Soil in Bojnourd, Iran. *Sustainability* **2023**, *15*, 3495. https://doi.org/10.3390/su15043495

Academic Editor: Teodor Rusu

Received: 28 January 2023
Revised: 4 February 2023
Accepted: 13 February 2023
Published: 14 February 2023

1. Introduction

The concentration of potentially harmful elements in soil is increasing worldwide due to increasing urbanization and progressive expansion of industrial sectors, which has sparked significant concern in several developing nations [1–3]. Due to the non-degradability and long residence time of HMs, urban soil has gradually become the critical sink and source of HM pollutants in urban ecosystems [4,5]. The major pollutants in cities are traffic emissions, heating and power plants, municipal waste, traffic and household

boilers. Against this background, the pollution level of HMs in surface soils may pose a critical risk to human health and the ecosystem [6,7]. Human exposure to HMs can occur through various routes, such as ingestion, inhalation, skin contact and accidental ingestion [8]. Therefore, many researchers have recently focused on the contamination of soils with HMs, the pollution processes and the identification of sources through various geostatistical techniques [7].

Despite extensive research on the content of HM in urban soils, it is still advisable to monitor and evaluate the levels of HM because the content of HM in soils is generally increasing [9]. To quantify the ecological risk assessment of HMs, environmental scientists have developed a variety of approaches in recent decades. The Geo-Accumulation Index (I_{geo}), the Comprehensive Ecological Risk Index (RI), the Single Pollution Index (P_i) and the Ecological Risks Index for Individual HMs (E_i) are all examples of such assessment indices [10–13]. Assessing the ecological risk of HMs in soil is critical for determining the extent of contamination and developing effective mitigation measures [14]. In addition to ecological risk assessment, human health risk assessment has recently attracted considerable interest because it has the potential to quantify the health risk of HM in soil [15]. Unfortunately, many nations lack their own national health risk assessment procedures and most of the studies conducted to date have instead relied heavily on the US Environmental Protection Agency (EPA) model and parameters [16]. Many studies have effectively assessed the human health risk posed by HMs in polluted soils using the USEPA approach, including those conducted in Poland [17], China [18], Chad, Africa [19], India [20], Turkey [21] and Brazil [22]. In addition, spatial distribution and heterogeneity of pollution status can also be assessed in great detail when these data are integrated with geographic information system technology (GIS) [23,24]. Considering this, there has been a wide variety of studies that have utilized both deterministic and geostatistical interpolation methods to determine soil HM spatial distributions. [25–29].

Antimony (Sb) has been a prominent focus of environmental concern since it is a naturally occurring, widely distributed and acutely hazardous environmental contaminant [30,31]. According to the United States Environmental Protection Agency and the European Union, Sb and its compounds are listed as priority pollutants in the Basel Convention's list of banned hazardous compounds [32]. Similar to Pb, Sb is also a cumulative toxicant [33]. In fact, these elements have relatively similar anthropogenic geochemical cycles and their environmental impacts are comparable in several cases [34]. Urban topsoil contains Sb in amounts of 0.05 mg·kg^{-1} to 73.20 mg·kg^{-1} (mean = 1.72 mg·kg^{-1}), representing its wide distribution. The Netherlands has recommended Sb target and intervention levels of 3.0 and 15.0 mg·kg^{-1} [35]. In Canada, the Sb target value is 20 mg·kg^{-1} for agricultural land, parks and residential areas [36]. Sb emissions into the environment have significantly increased as a result of using Sb alloys in various motor vehicle components, which is particularly evident in locations with high traffic density and with a substantially lower Cu/Sb ratio than the earth's crust [37]. The main sources of Sb in these areas are considered to be the abrasion of tires, brake pads and engine bearings, as well as the operation of the wheels, rails and cables of trains [38–40]. Other major sources of Sb in the environment include battery factories, waste dumps, flame retardants, coal combustion, bullet manufacturing and use, power plants and the automotive industry [41,42].

In environmental studies, certain aspects are considered depending on the types of contaminating metals, the level of pollution and the potential risk to human health [43]. In order to identify the source of pollution and mitigate the consequences of HMs on top-soils, these aspects are compared, analyzed and described [44]. In recent decades, numerous studies have been conducted on the effects of HM on urban soil and dust pollution, mostly near industrial areas, urban roads and streets [22,45–50]. According to the literature review, Sb concentration was the main topic of the few studies conducted worldwide. Thestorf and Makki [51] used an integrated geostatistical method to analyze the causes of soil Sb pollution in the Berlin metropolitan area. Their results show that the Sb content is significantly higher than in the natural environment. In addition, they found that Sb is a

significant pollutant that occurs exclusively in urban areas and has been neglected in the past. According to Földi et al. [41], Sb contamination of brake pads is detectable in roadside soils with a significant but negligible ecotoxicological potential for transfer into surface and groundwater.

Previous studies on HM urban soil pollution in Iran have mainly focused on risk assessment, spatial distribution, source identification and pollution level assessment across the country [43,44,52–54]; however, the concentration of Sb in urban soils is not well known. Dehghani et al. [55] investigated surface soils from the center of Tehran for important potentially hazardous elements. They reported that Sb had higher surface soil variation coefficients than street dust samples. They also found that only a small number of surface soils had high enrichment factor values for Sb, indicating strong element enrichment.

The establishment and implementation of urban environmental pollution indicators has become a valuable tool for public health policy and environmental protection management [56]. The ability to make decisions about the extent and technique of remediation or the option of not remediating at all is an outcome that could be measured as a result of conducting a risk analysis. In such situations, the permittee is required to take precautions to ensure that pollutants are controlled and that receptors are not at risk of exposure. Therefore, a risk assessment is required to meet these requirements [57].

This study used a systematic sampling approach to assess Sb, Cd, Cr and Pb levels in urban soil taken from Bojnourd. The primary aims were: (a) presenting geochemical maps of the considered elements in the field of study; (b) defining the natural or anthropogenic source of the chemical elements through combining multivariate statistics and GIS strategies and (c) assessing the potential hazard to both adult and child health; (d) to evaluate the HM levels in the soils of Bojnourd; (e) to understand hotspots and evaluate the potential origin of pollutants. In addition, this study is the basis for conducting future studies in larger cities in Iran.

2. Materials and Methods

2.1. Site Description and Sampling

Bojnourd city is situated in Northern Khorasan province, which spans an area of around 28,434 km^2, in northeastern Iran between 37°22′ and 37°58′ N and 57°05′ and 57°66′ E (Figure 1). High mountains, including Aladagh Mountain in the center and Kope-Dagh Zone in the north, surround this city. The average annual temperature in this area is 13.3 °C and the average annual rainfall is 272.4 mm, classifying it as a cold semi-arid (steppe) climate. In recent years, Bojnourd has undergone numerous territorial changes, including a sharp rise in population and urbanization, particularly following its selection as North Khorasan's provincial capital in 2004 [58]. Given that this city is among the province's most polluted cities, it is crucial to be informed of the influential factors in environmental pollution. After that, appropriate remediation strategies can be used to reduce and eventually eliminate these pollutants.

Firstly, using a systematic sampling distribution (900 × 900 m), 37 stations were determined for sampling from the urban surface soil. Based on the LUCAS methodology [59], at each station, one soil sample (0–20 cm) was collected (traffic areas, residential areas and suburbs) and, by using a Global Positioning System (GPS), each sampling location was recorded [60,61]. Figure 1 shows the study area, as well as the locations of the sampling points. A small plastic shovel was used to collect the soil samples. Then, each sample was placed in polyethylene bags, labelled and taken to the laboratory for further analysis.

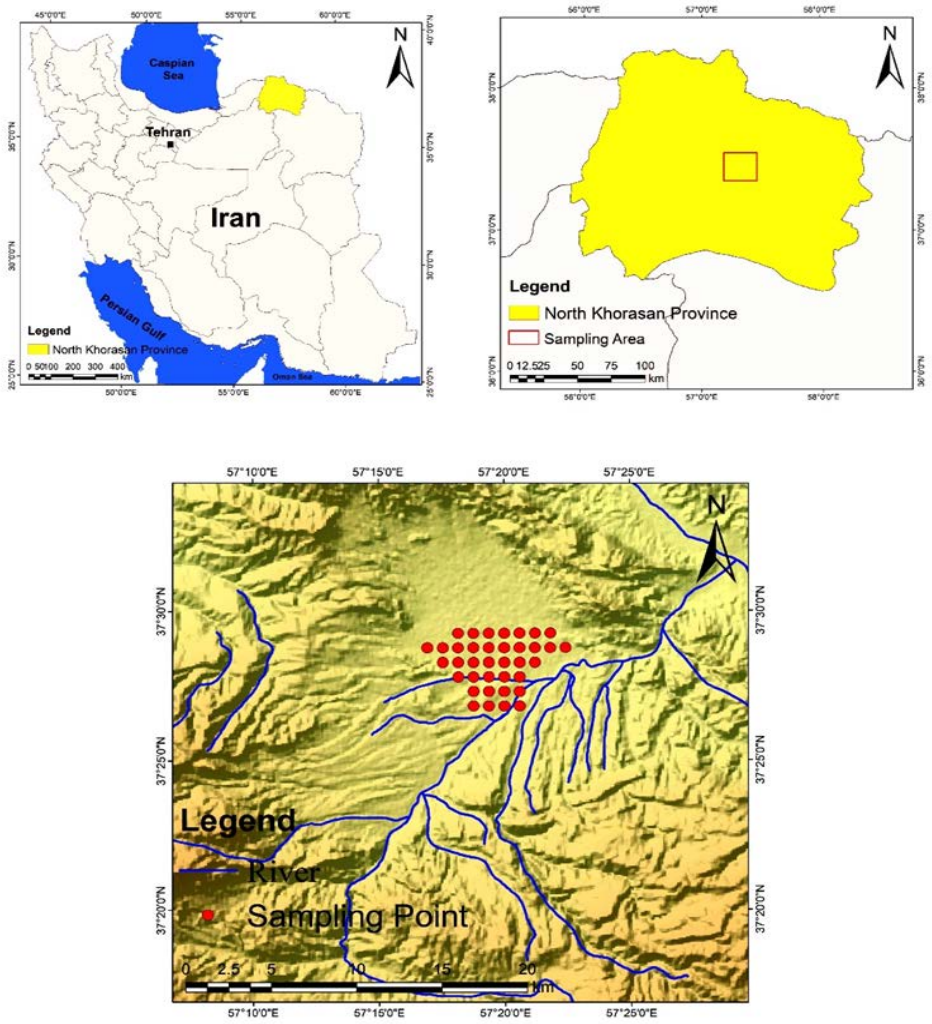

Figure 1. Map of study area and sampling stations.

2.2. Analytical Methods

Extraneous materials such as asphalt, paving stone, leaves, concrete and brick fragments and other materials were taken from the samples by sieving them through a 63 µmm sieve. Samples were then air dried, packed in polyethylene bags and labeled according to the procedures described by Tanner et al. [62]. According to USEPA [63], GB/T 17238-1997 and GB/T 17441-1997 [64,65], five grams of the soil samples were combined with highly purified nitric-hydrofluoric perchloric acids (4 mL HF, 2 mL $HClO_4$, 5 mL HNO_3). This was undertaken so that the samples could be digested and their HM contents could be determined. Finally, inductively coupled plasma-mass spectrometry was used to examine the content of HMs (ICP-MS, Hewlett-Packard, the USA). Furthermore, a pH meter was used to measure the soil's pH in a ratio of 1:2.5 soil to distilled water in terms of *w*/*w* (Jenway pH meter, 3540) [66].

2.3. HM Risk Assessment

2.3.1. Geo-Accumulation Index (I_{geo})

In 1969, Muller proposed the concept of geo-accumulation (I_{geo}). This index allows us to measure HM soil contamination in urban areas. Numerous studies have widely utilized it since 1969 [14,50,67]. The following Equation (1) was used to determine the Igeo:

$$\text{Igeo} = \log_2\left[\frac{\text{Cn}}{1.5\ \text{Bn}}\right] \quad (1)$$

where Cn is the content of the HM that was determined (mg·kg^{-1}) and Bn is the average value of the geochemical background for the measured HM (mg·kg^{-1}). A factor of 1.5 reduces the effect of potential alteration in the Bn values that emerged from a natural process. Muller classified the I_{geo} scheme into seven levels. The classification criteria are as follows: unpolluted, $I_{geo} < 0$; unpolluted to moderately polluted, $0 < I_{geo} \leq 1$; moderately polluted, $1 < I_{geo} \leq 2$; moderately to heavily polluted, $2 < I_{geo} \leq 3$; heavily polluted, $3 < I_{geo} \leq 4$; heavily to significantly polluted, $4 < I_{geo} \leq 5$; and significantly polluted, $I_{geo} > 5$ [68].

2.3.2. Contamination Factor (CF)

The Contamination factor (CF) can also be used to evaluate soil pollution. This index allows the evaluation of soil pollution, based on the content of HM from the surface soil presented by Håkanson [69] and it was considered using the following Equation (2):

$$CF = \frac{C_{metal}}{C_{background}} \quad (2)$$

where C_{metal} is the concentration of the HM that was evaluated in each sample (mg·kg^{-1}) and $C_{background}$ is the background content. The CF is generally classified into the following categories: slightly polluted (CF < 1), moderately polluted (1 < CF < 3), significantly polluted (3 < PI < 6) and very strong pollution (CF > 6) [70].

2.3.3. Health Risk Assessment

Prolonged exposure to toxic metals can have adverse impacts on human health and the United States Environmental Protection Agency (USEPA) has proposed a model for risk assessment to study and predict these effects [63,71]. Ingestion, skin contact (dermal exposure) and inhalation are the three potential routes of exposure that can be analyzed using this in-depth model. This makes it possible to assess carcinogenic as well as non-carcinogenic risks in both children and adults [63,71,72]. The average daily dose (ADD, mg·kg^{-1} day^{-1}) for metallic elements was estimated based on Equations (3)–(5) for ingestion, inhalation and dermal, respectively [71,73].

$$ADD_{ing} = \frac{C \times IngR \times EF \times ED}{BW \times AT} \times 10^{-6} \quad (3)$$

$$ADD_{inh} = \frac{C \times InhR \times EF \times ED}{PEF \times BW \times AT} \times 10^{-6} \quad (4)$$

$$ADD_{derm} = \frac{C \times SA \times AF \times ABS \times EF \times ED}{BW \times AT} \times 10^{-6} \quad (5)$$

where ADD ingestion, ADD inhalation and ADD dermal represent the average daily dose intake from ingestion, inhalation and dermal contact, respectively (mg·kg^{-1} day^{-1}). C represents the total HM concentration in the soil (mg·kg^{-1}); IngR (mg·day^{-1}) is the ingestion rate and InhR (m^3.day^{-1}) is the inhalation rate of soil particles; EF and ED are the exposure frequency (day/year) and exposure duration (year), respectively; BW is the exposed individual's average body weight (kg); AT (day) is average exposure time; SA, AF and ABS are the skin surface area (cm^2), the skin adherence factor (kg cm^2·d^{-1}) and the dermal absorption factor, respectively. Table S1 provides the values for the parameters.

Non-Carcinogenic and Carcinogenic Risk Assessment

The Hazard Index (HI) and the Carcinogenic Risk (CR) were utilized to evaluate the possible health risks posed by HMs [48]. In this study, the non-carcinogenic and carcinogenic health risks of soil HMs for each pathway were calculated as in [71,72,74,75] using the following Equations (6)–(9):

$$HQ = \frac{ADD_i}{RfD_i} \quad (6)$$

$$HI = \sum HQ_i \quad (7)$$

$$CR = ADD_i \times SF_i \quad (8)$$

$$TCR = \sum CR_i \quad (9)$$

where HQ is the non-carcinogenic risk quotient, which measures the non-carcinogenic hazard in every route; ADD_i is the cancer risk of a single contaminant through a single route; RfD is the reference dose (mg·kg^{-1} d^{-1}) of the pathway; HI is the overall non-cancer risk posed through many exposure pathways to a given pollutant. According to USEPA, if HQ_i or HI ≤ 1, no detrimental health impacts are detected; HQ_i or HI > 1 demonstrate the possibility of adverse health impacts. The carcinogenic risk (CR) indicates the potential of developing cancer risk due to multiple exposure pathways [71]. The slope coefficient (SF) is the cancer slope factor (mg·kg^{-1} day^{-1}). If CR is between 10^{-6}–10^{-4}, this indicates that the hazard is within acceptable limits; if the CR value is greater than 10^{-4}, this indicates that human tolerance is exceeded and when CR < 10^{-6}, this means that there is no health risk. All HM risk references of SF_i and RfD_i used in this study are based on Table S2.

2.4. Statistical Analysis

Statistical analysis, normal test (Kolmogorov–Smirnov) and correlation analysis of seven HMs were performed employing SPSS 21.0. Initially, the processing of data was conducted using descriptive statistics (including average, min-max range and standard deviation). In order to examine the differences in HM concentration between various types of land, a non-parametric Kruskal-Wallis test was run and then multiple comparisons were made post hoc. ArcGIS 10.6 was applied to create a map of the HMs' spatial distribution. As an interpolation method, the inverse distance weighted (IDW) method was chosen. Spearman's correlation was performed to evaluate the possible association among Sb and the other HMs. Excel 2019 was used to perform the calculations for the ecological and health risk assessments, as well as the construction of statistical graphics.

3. Results and Discussion

3.1. Descriptive Statistics of HMs in Soils

Interpretation of HM content is critically important for identifying potential effects on surrounding environments and community health for sustainable protection of the environment [76]. The descriptive statistics of Sb and other HMs (Cd, Cr, As, Ni, Hg and Pb) in soils of different land-use types and their background values are given in Table 1. The average pH of 8.04 for traffic areas (TA), 7.58 for residential areas (RA) and 7.54 for suburb areas (SA) suggested that the urban soil in the RA and SA was neutral, while TA was alkaline. We noticed a tendency for the gradual growth of pH values toward stations related to TA, which was consistent with the results found by Konstantinova et al. [77]. Moreover, the mean concentrations of Sb, Cd, Cr, As, Ni, Hg and Pb for TA were 4.72, 2.77, 59.04, 20.23, 52,6, 0.23 and 26.67 mg·kg^{-1}, respectively. The mean concentrations of the Sb, Cd, Cr, As, Ni, Hg and Pb for RA were observed to be 7.58, 1.79, 2.01, 46.97, 21.03, 35.64, 0.63 and 14.17 mg·kg^{-1}, respectively; while SA were 7.54, 0.92, 1.45, 39.42, 29.36, 30.81, 0.75 and 10.03 mg·kg^{-1}, respectively (Figure 2).

Table 1. Descriptive statistics of HMs in urban soils samples (mg·kg^{-1}).

Land Use	Parameter	pH	Sb	Cd	Cr	Pb	As	Ni	Hg
Traffic areas	Minimum Value	7.87	0.47	1.85	36.32	8.16	7.40	25.7	0.02
	Maximum Value	8.20	11.14	3.24	69.73	43.15	30.90	85	1.06
	Mean	8.04	4.72	2.77	59.04	26.67	20.23	52.6	0.23
	SD	0.09	3.69	0.51	9.17	9.83	6.36	16.24	0.31
Residential areas	Minimum Value	7.37	0.33	1.01	33.89	5.11	12.90	20.50	0.06
	Maximum Value	7.76	6.24	3.11	56.93	22.89	33.75	49.1	1.20
	Mean	7.58	1.79	2.01	46.97	14.17	21.03	35.64	0.63
	SD	0.13	2.03	0.57	7.91	5.59	6.53	8.83	0.37
Suburb areas	Minimum Value	7.36	0.32	0.56	30.35	4.33	13	17.50	0.07
	Maximum Value	7.66	2.91	2.09	55.75	28.01	57	46	1.43
	Mean	7.54	0.92	1.45	39.42	10.03	29.36	30.81	0.75
	SD	0.09	0.69	0.58	7.51	7.58	13.64	9.53	0.40

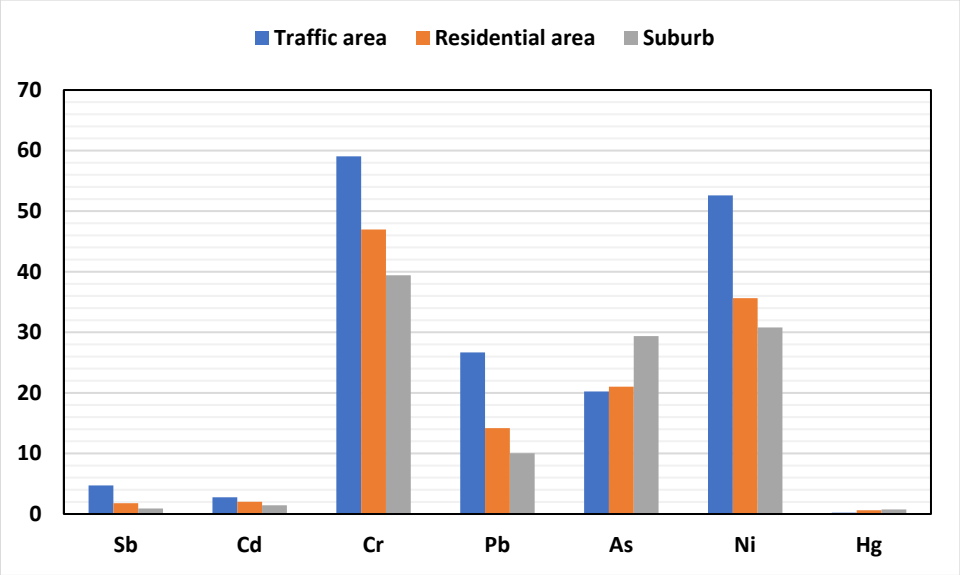

Figure 2. The mean concentrations of HMs (mg·kg^{-1}).

Comparisons were made between the HM contents measured in the soil samples and recommended soil quality guidelines in the Netherlands and Canada, as well as urban soils from Africa, India and China (Table 2). Accordingly, the mean Sb concentration in RA and SA was lower than the Dutch soil standard, while it was higher in TA. The mean concentrations of Pb and Cr in the Bojnourd soil samples are lower than those in Chinese and African urban soils and in Canadian and Dutch standard soils. Cr content was considerably lower than in Indian urban soils. The mean concentrations of Pb, As, Ni and Cr in TA and RA are higher than those in global soils. It is also noticeable that the concentration of Pb, As and Ni in TA is higher than that in Indian urban soils. The average Cd concentration in the soil samples is lower than that in African urban soils and Canadian standard soils, while the Cd and Ni concentrations in TA and RA are higher than those in global and Chinese urban soils and in Canadian and Dutch standard soils. Compared with Chinese urban soils and Dutch standard soils, the average Hg concentration in TA is lower, but the concentrations in RA and SA are higher. The content of HMs in SA is lower than most standards, except for As.

According to Utermann et al. [78], the pseudo-total background value of Sb for surface soils containing natural background material is 0.80 mg·kg^{-1} on average. Therefore, this study indicates that Sb most likely impacts the urban soil samples of the Bojnourd, contributed by anthropogenic sources. The mean concentrations of Sb in soils from some stations related to RA and SA were lower than the background values, while concentrations in TA exceeded these values. This finding was consistent with those of Thestorf and Makki [51], who found that Sb contents and other HM contents in the soils of Berlin decreased in suburban areas. They concluded that an elevated level of Sb is more likely to occur along the streets, channels, railway lines and residential and industrial areas. The lower Sb content in RA and SA confirms that the Sb concentration in urban soils is primarily derived from the parent material. The source of Sb in TA is probably heavy traffic, car tires and brake abrasion. In the western (Gorgan Road) and southeastern (Esfarayen and Mashhad Road) parts of Bojnourd city, roads were scratched, which increased the wear of asphalt tires. Statistical analysis showed that the concentration decreased with increasing distance from TA, which means that there is a significant relationship between pseudo-total Sb and distance, which proves traffic emissions as the main cause. The results of pseudo-total Sb concentrations in Bojnourd soils agreed with those of Foeldi et al. [41], who indicated that Sb accumulates strongly in the soil of TA due to emissions from vehicles and the content decreases with increasing distance from TA. In addition, they reported that the main source of such pollution is probably abrasion from tires and brake pads. We also observed that the Sb concentration decreased with increasing distance, almost to SA and the natural background levels: 0.92 mg·kg^{-1} (SA) and 0.45 mg·kg^{-1} (background), respectively.

Over recent decades, there has been a concurrent rise in the population of Bojnourd, which has led to an increase in the number of motor vehicles in the city. Consequently, solid particles from tire abrasion, exhaust fumes, brake pad wear and road surface abrasion have significantly increased the levels of Sb, Cd, Pb, Ni and other HMs in the soil. The study area showed higher HM levels compared to the background, which suggests that it has been contaminated by human activities. Various sources of pollution, such as human activities and traffic, have contributed to the gradual accumulation of Cd, Cr, Pb, Ni and Sb in the soils over time. Similar findings were reported by Wang and Lu [79] and Yan et al. [80]. The total Cd concentrations of some stations related to the SA were under 1.0 mg·kg^{-1}. In this regard, Kabata-Pendias [81] reported that the contents of Cd do not exceed 1.0–1.1 mg·kg^{-1} for most surface soils around the world. Therefore, the values in SA possibly represent pedogeochemical backgrounds. However, the mean concentrations of As (29.36 mg·kg^{-1}) and Hg (0.75 mg·kg^{-1}) in SA were higher than in other land types. As mentioned by Okoye et al. [82], As is utilized in the production of pesticides and has other industrial applications. Most of the soil samples taken from SA were on agricultural land and near industrial facilities, which may be the reason for the elevated levels of this element. Human activities are the main contributors to Hg emissions, with the majority coming from urban agglomerations, waste incinerators, coal-fired power plants and metal smelters [83].

Higher average Pb content (26.67 mg·kg^{-1}) was measured along traffic routes in TA, which was directly related to pollution from car exhaust. TA was influenced by excessive traffic activities as well as vehicle exhaust and other components that contributed significantly to Pb dispersion. Morera-Gómez et al. [47] reported Pb concentration in urban soils from Cuba, which is in agreement with our results, and found a high degree of pollution for this element. In addition, the high level of Cr and Cd in the study area is probably due to brakes and tires. In addition, Cr is also released from concrete due to construction activities. Zhang et al. [84] reported a similar finding in the roadside soil of Urumqi City.

Antimony replaced asbestos in brake pads in the late 1980s [85], which was a major concern because of PM2.5 and PM10 aerosols containing Sb emitted by vehicles, as well as the potential cancer risk of Sb_2S_3 [86,87]. One of the main sources of Pb is brake pad abrasion [88], which is widely recognized as a substantial hazardous gasoline additive [89,90]. Since the early 2000s, Iran has banned the addition of Pb to gasoline. Nevertheless, Pb has accumulated in the urban environment over time due to its extended half-life and low leaching from soil [91,92].

Table 2. Guideline values based on local background and references ($mg \cdot kg^{-1}$).

Origin	Sb	Cd	Cr	Pb	As	Ni	Hg	Reference
World soils	-	1.1	42	14	4.7	18	-	CEPA [93]
Indian urban soils	-	-	211.16	16.715	9.9	52.46	-	Adimalla [7]
Dutch soil quality guidelines	3	0.8	100	100	29	35	0.3	VROM [35]
Canadian soil quality	-	22	87	87	12	50	-	CEPA [93]
Chinese urban soils	-	1.8	122	187	14	42	0.26	Pecina et al. [48]
African urban soils	-	5	250	150	-	100	-	Yabe et al. [94]
Soil geochemical background	0.45	0.33	30.07	3.45	8.59	33.45	0.068	This study

Earlier studies have found that the concentration of HM in soils is strongly influenced by the different types of land uses, particularly those that include a wide variety of human activities [95]. Traffic areas are considered as HM sources, especially for Cd and Pb [96,97]. Findings suggest that roadside soils are significantly contaminated by Ni, Zn, Pb, Cd and Cr [97,98]. The concentrations of HMs in TA were higher than those in RA, SA and the background levels, showing how the distance from roads affects the distribution of HM in urban soils [99]. Consistent with the findings of Li et al. [99], our investigation found that soil HM concentrations reduced with increasing distance from roads and streets. Comparing the content of soil HMs throughout different land use types also revealed that HM concentrations were significantly affected by the land use type and human activities in the study area. In this study, with regard to the mean concentrations of the studied elements, SA had the lowest values, followed by RA. TA is associated with stations located mainly in the center, south, southeast and west.

3.2. Spatial Distribution of HMs

In order to detect spots with high and low concentrations of soil HMs, a geochemical map is an indispensable tool [2,100]. The inverse distance weighted (IDW) approach was applied to obtain spatial distribution maps of Sb, Ni, As, Cr, Hg, Cd and Pb in urban surface soils. All maps are presented in Figure 3. Sb, Cd, Ni and Cr all exhibited a similar distribution pattern in that their concentrations were higher in the center, west and south-eastern directions of the Bojnourd city, while the south-eastern and western regions have the highest concentration of Pb. In these parts of the city, the major highway with several roadways and transit hubs with bus terminals are situated; consequently, the contamination of HMs appears to be derived from vehicle emissions. Due to the decline in the volume of traffic/vehicle emissions, Sb concentrations reduced in the northern section of the study area. In addition, As and Hg showed a similar pattern in that their main concentrations were in the southeast and north-eastern of the city, which is mainly located in SA.

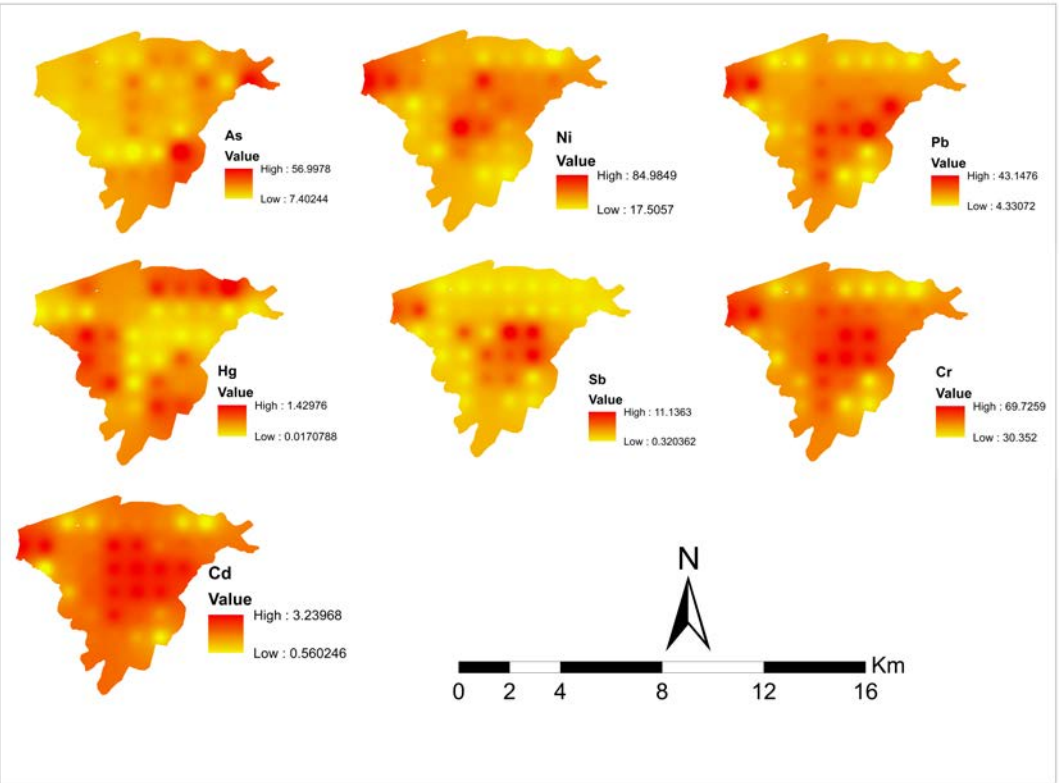

Figure 3. Spatial distribution of HMs in the surface soils of the study area (mg·kg^{-1}).

3.3. Ecological Risk Assessment

The geo-accumulation (I_{geo}) model is extensively used to estimate the extent of soil HM pollution [68,101,102]. Using the geo-accumulation index, the levels of Sb, Cd, Cr, As, Ni, Hg and Pb pollution in the study area soils were determined. Table 3 summarizes the findings. The highest I_{geo} values of Sb (2.14), Cd (2.46) and Pb (2.49) were found in TA soil samples, indicating a moderately to heavily polluted level. Hoshyari et al. [29] also made a similar finding. The I_{geo} values for Ni and Cr in all sampling stations and Sb in RA and SA were smaller than 1, signifying that soil was viewed as unpolluted to moderately polluted. Meanwhile, the I_{geo} for Cd, As and Pb in RA and SA signifies a moderate contamination. Additionally, Hg was the most harmful element to the environment. The highest values of this element were estimated in RA (2.63) and SA (2.88), moderately to heavily polluted. Specifically, TA had the highest values of I_{geo} for the studied HMs, except for As and Hg, which is in agreement with the findings from Fei et al. [103]. Pb and Cd had moderately polluted the majority of monitoring stations' soils in Bojnourd.

Table 3. Contamination factor (CF) and geo-accumulation (I_{geo}) for four HMs in the study area.

HMs	Geo-Accumulation (I_{geo})			Contamination Factor (CF)		
	TA	RA	SA	TA	RA	SA
Pb	2.49	1.74	1.2	10.49	3.98	2.1
Cd	2.46	1.96	1.42	7.73	4.11	2.91
Cr	0.37	0.037	−0.22	8.4	6.1	4.39
Sb	2.14	0.76	0.21	1.97	1.57	1.32
As	0.65	0.71	1.19	2.35	2.45	3.41
Ni	0.07	−0.50	−0.70	1.57	1.1	0.92
Hg	1.17	2.63	2.88	3.38	9.26	11.03

The current study calculated the contamination factor (CF) for chosen HMs to estimate the pollution level and potential anthropogenic inputs in urban surface soil samples. Obtained CF values for individual HMs in soil samples are listed in Table 3. The CF values of the four HMs follow a declining order: Hg > Pb > Cr > Cd > As > Sb > Ni. The highest and lowest CF values were both found in the SA land type, 11.03 for Hg and 0.92 for Ni. Sb and Ni in the entire city display low contamination; thus, these HMs do not seem to be impacted by anthropogenic sources of pollution in soil samples. According to this index, As and Hg showed considerable to very strong pollution levels in RA and SA. Shrivastava et al. [104] and Majumdar et al. [105] also found a high level of As pollution in their investigation. The CF value for Cr, Pb and Cd indicated a considerable pollution level in RA, whereas the CF values for those HMs in the TA soil samples indicated extreme contamination levels, suggesting that soil in the study area was highly polluted by human-induced activities.

3.4. Multivariate Analysis of HMs in Soil

The Spearman correlation between HMs contents in soil samples from Bojnourd is displayed in Table 4. The Kolmogorov–Smirnov test was applied to normalize the results of analyzed HMs. After the data were normalized, the inter-element relations between HMs were evaluated using Spearman correlation to identify possible HM sources and routes. Positive correlations were identified among Pb-Cd-Cr-Ni-Sb, indicating a common source for these HMs. Other studies have also reported a strong positive correlation between Cr-Cd-Pb [44,45]. Interestingly, Hg and As did not show any strong positive correlations with the other HMs, indicating they may come from a separate source. Zhang et al. [106] also found a similar result.

Table 4. Spearman correlation matrix of HMs in topsoil samples.

HM	Pb	Cd	Cr	Sb	As	Ni	Hg
Pb	1	0.884 **	0.891 **	0.803 **	−0.142	0.703 **	−0.682 **
Cd		1	0.915 **	0.830 **	−0.019	0.705 **	−0.685 **
Cr			1	0.837 **	−0.221	0.737 **	−0.722 **
Sb				1	−0.072	0.509 **	−0.520 **
As					1	−0.077	−0.013
Ni						1	−0.921 **
Hg							1

Note: ** $p < 0.01$.

3.5. Health Risk Assessment of HMs

In this investigation, the potential non-cancer and cancer hazards via ingestion, skin contact and inhalation of Sb, Pb, Ni, As, Cr, Hg and Cd in urban soil were evaluated for adults and children in the study area. The ADD via multiple pathways showed the disparity between the land types in Table S3. A summary of the research on the cancer and non-cancer effects of HMs in soils on adults and children is provided in Tables 5 and 6.

As shown in Table 5, for both children and adults, the HQ values for four HMs were ingestion > dermal > inhalation, showing that the primary exposure route for the whole study area was through ingestion, which was more in agreement with similar investigations [7,107]. Inhalation was the lowest exposure route for HQ, therefore it is unlikely to pose a greater risk than ingestion. This means that inhalation of HMs through the nose and mouth will be a less significant route of exposure than the others. The values of HQ and HI for different HMs followed the order: As > Cr > Sb > Pb > Cd > Ni > Hg.

Table 5. The results of non-cancer health risk evaluation from soil HMs.

HMs	Land Type	Adult				Children			
		HQing	HQinh	HQdermal	HI	HQing	HQinh	HQdermal	HI
Sb	TA	1.62×10^{-2}	-	-	1.62×10^{-2}	1.51×10^{-1}	-	-	1.51×10^{-1}
	RA	6.13×10^{-3}	-	-	6.13×10^{-3}	5.72×10^{-2}	-	-	5.72×10^{-2}
	SA	3.15×10^{-3}	-	-	3.15×10^{-3}	2.94×10^{-2}	-	-	2.94×10^{-2}
Cd	TA	3.8×10^{-3}	7.49×10^{-6}	1.55×10^{-3}	5.32×10^{-3}	3.54×10^{-2}	5.69×10^{-7}	9.92×10^{-3}	4.54×10^{-2}
	RA	2.74×10^{-3}	5.44×10^{-6}	1.1×10^{-3}	3.86×10^{-3}	2.57×10^{-2}	4.13×10^{-7}	7.2×10^{-3}	3.29×10^{-2}
	SA	1.99×10^{-3}	3.92×10^{-6}	7.93×10^{-4}	2.79×10^{-3}	1.85×10^{-2}	2.98×10^{-7}	5.2×10^{-3}	2.38×10^{-2}
Cr	TA	2.71×10^{-2}	0.000319	5.38×10^{-3}	3.27×10^{-2}	2.52×10^{-1}	2.42×10^{-5}	3.52×10^{-2}	2.87×10^{-1}
	RA	2.15×10^{-2}	0.000254	4.28×10^{-3}	2.6×10^{-2}	2.01×10^{-1}	1.93×10^{-5}	2.81×10^{-2}	2.28×10^{-1}
	SA	1.8×10^{-2}	0.000213	3.6×10^{-3}	2.18×10^{-2}	1.68×10^{-1}	1.62×10^{-5}	2.35×10^{-2}	1.92×10^{-1}
Pb	TA	1.05×10^{-2}	1.17×10^{-6}	2.78×10^{-4}	1.07×10^{-2}	9.74×10^{-2}	8.89×10^{-8}	1.82×10^{-3}	9.93×10^{-2}
	RA	5.55×10^{-3}	6.22×10^{-7}	1.48×10^{-4}	5.7×10^{-3}	5.18×10^{-2}	4.72×10^{-8}	9.66×10^{-4}	5.27×10^{-2}
	SA	3.93×10^{-3}	4.4×10^{-7}	1.04×10^{-4}	4.03×10^{-3}	3.67×10^{-2}	3.34×10^{-8}	6.84×10^{-4}	3.73×10^{-2}
As	TA	4.75×10^{-2}	4.75×10^{-2}	3.96×10^{-2}	1.34×10^{-1}	4.43×10^{-1}	1.24×10^{-11}	3.18×10^{-2}	4.75×10^{-1}
	RA	4.92×10^{-2}	7.26×10^{-12}	4.12×10^{-2}	9.06×10^{-2}	4.61×10^{-1}	1.29×10^{-11}	3.31×10^{-2}	4.94×10^{-1}
	SA	6.89×10^{-2}	1.01×10^{-11}	5.75×10^{-2}	1.26×10^{-1}	6.43×10^{-1}	1.8×10^{-11}	4.61×10^{-2}	6.90×10^{-1}
Ni	TA	1.85×10^{-3}	2.1×10^{-13}	7.82×10^{-5}	1.93×10^{-3}	1.73×10^{-2}	3.72×10^{-13}	6.28×10^{-5}	1.73×10^{-2}
	RA	1.25×10^{-3}	1.42×10^{-13}	5.3×10^{-5}	1.31×10^{-3}	1.17×10^{-2}	2.52×10^{-13}	4.25×10^{-5}	1.17×10^{-2}
	SA	1.08×10^{-3}	1.23×10^{-13}	4.58×10^{-5}	1.13×10^{-3}	1.01×10^{-2}	2.18×10^{-13}	3.68×10^{-5}	1.02×10^{-2}
Hg	TA	5.40×10^{-4}	2.78×10^{-13}	8.8×10^{-5}	6.28×10^{-4}	5.04×10^{-3}	4.93×10^{-14}	7.06×10^{-5}	5.11×10^{-3}
	RA	1.48×10^{-3}	7.62×10^{-13}	2.41×10^{-4}	1.72×10^{-3}	1.38×10^{-2}	1.35×10^{-12}	1.93×10^{-4}	1.40×10^{-2}
	SA	1.76×10^{-3}	9.07×10^{-13}	2.87×10^{-4}	2.05×10^{-3}	1.64×10^{-2}	1.61×10^{-12}	2.30×10^{-4}	1.67×10^{-2}

Table 6. The results of cancer health risk evaluation from soil HMs.

HMs	Land Type	Adult				Children			
		CRng	CRinh	CRdermal	TCR	CRng	CRinh	CRdermal	TCR
Cd	TA	2.31×10^{-5}	2.69×10^{-9}	9.24×10^{-8}	2.32×10^{-5}	2.16×10^{-4}	2.05×10^{-10}	6.05×10^{-7}	2.17×10^{-4}
	RA	1.68×10^{-5}	1.96×10^{-9}	6.7×10^{-8}	1.69×10^{-5}	1.57×10^{-4}	1.49×10^{-10}	4.39×10^{-7}	1.57×10^{-4}
	SA	1.21×10^{-5}	1.41×10^{-9}	4.83×10^{-8}	1.22×10^{-5}	1.13×10^{-4}	1.07×10^{-10}	3.17×10^{-7}	1.13×10^{-4}
Cr	TA	4.04×10^{-5}	3.83×10^{-7}	6.45×10^{-6}	4.73×10^{-5}	3.77×10^{-4}	2.91×10^{-8}	4.23×10^{-5}	4.2×10^{-4}
	RA	3.22×10^{-5}	3.05×10^{-7}	5.13×10^{-6}	3.76×10^{-5}	3×10^{-4}	2.32×10^{-8}	3.36×10^{-5}	3.34×10^{-4}
	SA	2.7×10^{-5}	2.56×10^{-7}	4.31×10^{-6}	3.16×10^{-5}	2.52×10^{-4}	1.94×10^{-8}	2.82×10^{-5}	2.8×10^{-4}
Pb	TA	3.11×10^{-7}	1.73×10^{-10}	1.24×10^{-12}	3.11×10^{-7}	2.9×10^{-6}	1.31×10^{-11}	8.12×10^{-12}	2.9×10^{-6}
	RA	1.65×10^{-7}	9.19×10^{-11}	6.58×10^{-13}	1.65×10^{-7}	1.54×10^{-6}	6.98×10^{-12}	4.31×10^{-12}	1.54×10^{-6}
	SA	1.17×10^{-7}	6.5×10^{-11}	4.66×10^{-13}	1.17×10^{-7}	1.09×10^{-6}	4.94×10^{-12}	3.05×10^{-12}	1.09×10^{-6}
As	TA	7.33×10^{-6}	1.08×10^{-14}	6.12×10^{-6}	1.34×10^{-5}	1.71×10^{-5}	4.78×10^{-15}	1.23×10^{-6}	1.83×10^{-5}
	RA	7.62×10^{-6}	1.12×10^{-14}	6.36×10^{-6}	1.4×10^{-5}	1.78×10^{-5}	6.76×10^{-6}	1.28×10^{-6}	2.58×10^{-5}
	SA	1.06×10^{-5}	1.56×10^{-14}	8.88×10^{-6}	1.95×10^{-5}	2.48×10^{-5}	6.94×10^{-15}	1.78×10^{-6}	2.66×10^{-5}
Ni	TA	1.16×10^{-5}	1.57×10^{-15}	6.16×10^{-6}	1.77×10^{-5}	2.7×10^{-5}	6.96×10^{-16}	1.23×10^{-6}	2.82×10^{-5}
	RA	7.83×10^{-6}	1.06×10^{-15}	4.17×10^{-6}	1.2×10^{-5}	1.83×10^{-5}	4.71×10^{-16}	8.37×10^{-7}	1.91×10^{-5}
	SA	6.77×10^{-6}	9.19×10^{-15}	3.61×10^{-6}	1.04×10^{-5}	1.58×10^{-5}	4.08×10^{-16}	7.23×10^{-7}	1.65×10^{-5}

In the study area, As exhibited the highest HQ value among these seven HMs for the ingestion route in both children and adults, while compared to inhalation the dermal

contact pathway was more hazardous for both age groups. In the present study, HQ and HI values through three exposure pathways exposed to HMs for adults were less than for children. This finding implies that non-carcinogenic risks are more severe for children than for adults due to all three mentioned exposures. Recent studies have also found that the two main factors contributing to children's health risks are increased soil ingestion and lower body weight [2,108]. Furthermore, the HQ and HI values for both adults and children are less than 1, suggesting that the seven examined HMs pose no non-carcinogenic health risk. However, the HI values of Cr and As for children were very close to the recommended value of 1; as a result, paying proper attention to these elements and children's health is critical. These findings support the results of Tyagi et al. [109], Li et al. [110], Huang et al. [111] and Wu et al. [112]. Ghani et al. [113] and Shen et al. [114] indicated that, for both children and adults, ingestion is the main route of exposure, which is associated with soil particles being in suspension and with hand-to-mouth contact.

Table 6 shows the calculated cancer risks only for the five HMs (Pb Cr, As, Ni, Cd and As), because the carcinogenic slope factors for Sb and Hg were not available. It has shown that the CR and TCR values of Pb, Cr, Ni, Cd and As for children and adults are still categorized as ingestion > dermal > inhalation. The total carcinogenic risk (TCR) of Cd, Cr, As, Ni and Pb to adults ranged from 1.22×10^{-5} to 2.32×10^{-5}, 3.16×10^{-5} to 4.73×10^{-5}, 1.34×10^{-5} to 1.95×10^{-5}, 1.04×10^{-5} to 1.77×10^{-5} and 1.17×10^{-7} to 3.11×10^{-7}, respectively, and for children 1.13×10^{-4} to 2.17×10^{-4}, 2.8×10^{-4} to 4.2×10^{-4}, 1.83×10^{-5} to 2.66×10^{-5}, 1.65×10^{-5} to 2.82×10^{-5} and 1.09×10^{-6} to 2.8×10^{-4}, respectively. The CR values increased as follows: Pb < Ni < As < Cd < Cr for adults and children. The TCR values indicated that the carcinogenic risks associated with Ni and As in soil were within the permissible limit for both adults and children. In addition, the total TCR and CR ingestion values of all HMs (except Pb) for adults were 10^{-5}, which show acceptable risk. Since the TCR and CR were below the 1.00×10^{-4} threshold range, it implies that there is no detectable cancer threat for adults in the study area due to carcinogenic HMs. However, children seemed more susceptible to health risks associated with chronic health problems than adults, according to carcinogenic HMs. Only the CR values of Cr and Cd for children through ingestion surpassed the acceptable risk level of 1.00×10^{-4}. In children, the calculated CR values for Pb were below the acceptable risk level. Moreover, TCR values of Cr and Cd for children were higher than 1×10^{-4}, which was a significant cancer risk. Bineshpour et al. [44] reported that, in Arak surface soil, children were shown to have a higher cancer risk from HMs than adults. Several other investigations have confirmed the same findings [115–117].

4. Conclusions

Exposure to different concentrations of Sb may lead to a variety of diseases, cancers and genetic defects in humans. In this study, the concentration levels, geo-accumulation index, contamination factor, human health risk and spatial distribution of Sb, Ni, As, Cr, Hg, Cd and Pb in the top-soil of Bojnourd were investigated. The mean concentrations of these HMs in the surface soil were higher than their background levels, indicating that this contamination may be of anthropogenic origin. Cd, Cr and Pb showed extreme CF values in RA, while Sb indicated the lowest CF value in all sampling stations. According to I_{geo}, a large part of the study area was moderately contaminated by Pb and Cd. Pearson's correlation coefficient confirmed that all HMs showed a strong positive correlation, indicating a common source, except for As and Hg. Geo-statistics and GIS methods were employed in order to generate the spatial distribution maps of the HM contents. A similar spatial distribution trend was found for Ni, Cr, Cd and Sb, with hot-spot areas correlated with the city center, the west and the southeast of the city.

Human health risk assessment of HMs in soil samples revealed that ingestion caused the greatest risk, followed by skin contact and inhalation. In the soil samples from Bojnourd, children have higher non-carcinogenic HQi levels for potentially hazardous metals than adults. The values of HQ and HI were lower than 1 for each metal, indicating no

noncarcinogenic risk for either age group. For adults and children, the cancer risk of Pb did not exceed the permissible limit of 1.0×10^{-6}, whereas the cancer risk for children was serious for Cd and Cr. The carcinogenic risks of Cd and Cr for adults in the region were also within acceptable limits. This study is useful and informative for the residents, especially children, and for the authorities to take proper precautions in order to ensure the safety of Bojnourd residents from this metal (Sb), which is almost unknown in Iran.

Supplementary Materials: The following supporting information can be downloaded at: https://www.mdpi.com/article/10.3390/su15043495/s1, Table S1: Values of factors used in the risk assessment formulae; Table S2: Reference dose (RfD) and slope factor (SF) of heavy metals for health risk assessment; Table S3: Heavy metal average daily dose (ADD) by oral, dermal and inhalation exposure routes among children and adults. References [118–126] are cited in the supplementary materials.

Author Contributions: Conceptualization: A.R.: Study conception and design, Data collection, analysis and interpretation of results, Supervision, Writing—original draft, Writing—review & editing. M.M.: Writing—original draft, Writing—review & editing. M.H.: Writing—original draft, Writing—review & editing. R.S.: Data collection, analysis and interpretation of results and Funding. M.Z.G.: Writing—review & editing. All authors have read and agreed to the published version of the manuscript.

Funding: This research received no external funding.

Institutional Review Board Statement: Not applicable.

Informed Consent Statement: Not applicable.

Data Availability Statement: The datasets generated during this study are presented in the tables in this manuscript and in the supplementary material.

Conflicts of Interest: The authors have no conflict of interest to declare that are relevant to the content of this article.

References

1. Baltas, H.; Şirin, M.; Gökbayrak, E.; Ozcelik, A.E. A case study on pollution and a human health risk assessment of heavy metals in agricultural soils around Sinop province, Turkey. *Chemosphere* **2019**, *241*, 125015. [CrossRef] [PubMed]
2. Jiang, H.; Cai, L.; Wen, H.; Hu, G.; Chen, L.; Luo, J. An integrated approach to quantifying ecological and human health risks from different sources of soil heavy metals. *Sci. Total Environ.* **2019**, *701*, 134466. [CrossRef]
3. Shojaee Barjoee, S.; Malverdi, E.; Kouhkan, M.; Alipourfard, I.; Rouhani, A.; Farokhi, H.; Khaledi, A.A. Health assessment of industrial ecosystems of Isfahan (Iran) using phytomonitoring: Chemometric, micromorphology, phytoremediation, air pollution tolerance and anticipated performance indices. *Urban Clim.* **2023**, *48*, 101394. [CrossRef]
4. Gu, Y.; Gao, Y.; Lin, Q. Contamination, bioaccessibility and human health risk of heavy metals in exposed-lawn soils from 28 urban parks in southern China's largest city, Guangzhou. *Appl. Geochem.* **2016**, *67*, 52–58. [CrossRef]
5. Lu, X.; Wang, L.; Li, L.; Lei, K.; Huang, L.; Kang, D. Multivariate statistical analysis of heavy metals in street dust of Baoji, NW China. *J. Hazard. Mater.* **2010**, *173*, 744–749. [CrossRef]
6. Różański, S.Ł.; Castejón, J.M.P.; McGahan, D.G. Child risk assessment of selected metal(loid)s from urban soils using in vitro UBM procedure. *Ecol. Indic.* **2021**, *127*, 107726, ISSN 1470-160X. [CrossRef]
7. Adimalla, N. Heavy metals pollution assessment and its associated human health risk evaluation of urban soils from Indian cities: A review. *Environ. Geochem. Health* **2019**, *42*, 173–190. [CrossRef]
8. Han, X.; Lu, X.; Zhang, Q.; Wuyuntana Hai, Q.; Pan, H. Grain-size distribution and contamination characteristics of heavy metal in street dust of Baotou, China. *Environ. Earth Sci.* **2016**, *75*, 1–10. [CrossRef]
9. Dąbkowska-Naskręt, H.; Różański, S.; Bartkowiak, A. Forms and mobility of trace elements in soils of park areas from the city of Bydgoszcz, north Poland. *Soil Sci. Annu.* **2016**, *67*, 73. [CrossRef]
10. Li, Z.; Ma, Z.; Kuijp, T.; Yuan, Z.; Huang, L. A review of soil heavy metal pollution from mines in China: Pollution and health risk assessment. *Sci. Total. Environ.* **2014**, *468–469*, 843–853. [CrossRef]
11. Hu, B.; Shao, S.; Ni, H.; Fu, Z.; Hu, L.; Zhou, Y.; Min, X.; She, S.; Chen, S.; Huang, M.; et al. Current status, spatial features, health risks, and potential driving factors of soil heavy metal pollution in China at province level. *Environ. Pollut.* **2020**, *266*, 114961. [CrossRef]
12. Baruah, S.; Ahmed, I.; Das, B.; Ingtipi, B.; Boruah, H.; Gupta, S.; Nema, A.; Chabukdhara, M. Heavy metal(loid)s contamination and health risk assessment of soil-rice system in rural and peri-urban areas of lower Brahmaputra valley, Northeast India. *Chemosphere* **2020**, *266*, 129150. [CrossRef]

13. Gujre, N.; Mitra, S.; Soni, A.; Agnihotri, R.; Rangan, L.; Rene, E.; Sharma, M. Speciation, contamination, ecological and human health risks assessment of heavy metals in soils dumped with municipal solid wastes. *Chemosphere* **2021**, *262*, 128013. [CrossRef]
14. Liu, P.; Hu, W.; Tian, K.; Huang, B.; Zhao, Y.; Wang, X.; Zhou, Y.; Shi, B.; Kwon, B.; Ryu, J.; et al. Accumulation and ecological risk of heavy metals in soils along the coastal areas of the Bohai Sea and the Yellow Sea: A comparative study of China and South Korea. *Environ. Int.* **2020**, *137*, 105519. [CrossRef]
15. Sun, J.; Zhao, M.; Huang, J.; Liu, Y.; Wu, Y.; Cai, B.; Han, Z.; Huang, H.; Fan, Z. Determination of priority control factors for the management of soil trace metal (loid)s based on source-oriented health risk assessment. *J. Hazard. Mater.* **2021**, *423*, 127116. [CrossRef]
16. Yang, S.; Sun, L.; Sun, Y.; Song, K.; Qin, Q.; Zhu, Z.; Xue, Y. Towards an integrated health risk assessment framework of soil heavy metals pollution: Theoretical basis, conceptual model, and perspectives. *Environ. Pollut.* **2023**, *316*, 120596. [CrossRef]
17. Świdwa-Urbańska, J.; Batlle-Sales, J. Data quality oriented procedure, for detailed mapping of heavy metals in urban topsoil as an approach to human health risk assessment. *J. Environ. Manag.* **2021**, *295*, 113019. [CrossRef]
18. Liang, J.; Liu, Z.; Tian, Y.; Shi, H.; Fei, Y.; Qi, J.; Mo, L. Research on health risk assessment of heavy metals in soil based on multi-factor source apportionment: A case study in Guangdong Province, China. *Sci. Total Environ.* **2023**, *858*, 159991. [CrossRef]
19. Ajani, M.; Maleka, P.P.; Penabei, S.; Usman, I.T. Health risk assessment of heavy metals concentration from soil; a case study of the Mayo-Dallah in Southern area of Chad. *J. Radiat. Res. Appl. Sci.* **2022**, *15*, 130–138. [CrossRef]
20. Kumar, S.; Prasad, S.; Shrivastava, M.; Bhatia, A.; Islam, S.; Yadav, K.K.; Kharia, S.K.; Dass, A.; Gupta, N.; Yadav, S.; et al. Appraisal of probabilistic levels of toxic metals and health risk in cultivated and marketed vegetables in urban and peri-urban areas of Delhi, India. *Environ. Toxicol. Pharmacol.* **2022**, *92*, 103863. [CrossRef]
21. Yüksel, B.; Ustaoğlu, F.; Tokatlı, C.; Islam, M.S. Ecotoxicological risk assessment for sediments of Çavuşlu stream in Giresun, Turkey: Association between garbage disposal facility and metallic accumulation. *Environ. Sci. Pollut. Res.* **2022**, *29*, 17223–17240. [CrossRef]
22. Penteado, J.; Brum, R.D.; Ramires, P.F.; Garcia, E.M.; Santos, M.D.; Júnior, F.M. Health risk assessment in urban parks soils contaminated by metals, Rio Grande city (Brazil) case study. *Ecotoxicol. Environ. Saf.* **2021**, *208*, 111737. [CrossRef] [PubMed]
23. Pan, C.; Yu, F.; Tao, X.; Guo, J.; Yu, Y. Contamination, spatial distribution and source analysis of heavy metals in surface soil of Anhui Chaohu Economic Development Zone, China. *Sustainability* **2020**, *12*, 8117. [CrossRef]
24. Xu, X.; Zhang, X.; Peng, Y.; Li, R.; Liu, C.; Luo, X.; Zhao, Y. Spatial distribution and source apportionment of agricultural soil heavy metals in a rapidly developing area in East China. *Bull. Environ. Contam. Tox.* **2021**, *106*, 33–39. [CrossRef] [PubMed]
25. Lyla, P.S.; Manokaran, S.; Ajmalkhan, S.; Ansari, K.G.; Raja, S.; Reshi, O.R. Spatial distribution, ecological risk assessment, control factors, and sources of heavy metal pollution in the shelf surface sediments of the southwest Bay of Bengal, India. *Reg. Stud. Mar. Sci.* **2022**, *56*, 102705. [CrossRef]
26. Xiang, Q.; Yu, H.; Chu, H.; Hu, M.; Xu, T.; Xu, X.; He, Z. The potential ecological risk assessment of soil heavy metals using self-organizing map. *Sci. Total Environ.* **2022**, *843*, 156978. [CrossRef]
27. Saha, A.; Gupta, B.S.; Patidar, S.; Martínez-Villegas, N. Spatial distribution based on optimal interpolation techniques and assessment of contamination risk for toxic metals in the surface soil. *J. S. Am. Earth Sci.* **2022**, *115*, 103763. [CrossRef]
28. Zheng, F.; Guo, X.; Tang, M.; Zhu, D.; Wang, H.; Yang, X.; Chen, B. Variation in pollution status, sources, and risks of soil heavy metals in regions with different levels of urbanization. *Sci. Total Environ.* **2023**, *866*, 161355. [CrossRef] [PubMed]
29. Hoshyari, E.; Hassanzadeh, N.; Keshavarzi, B.; Jaafarzadeh, N.; Rezaei, M. Spatial distribution, source apportionment, and ecological risk assessment of elements (PTEs, REEs, and ENs) in the surface soil of shiraz city (Iran) under different land-use types. *Chemosphere* **2023**, *311 Pt 1*, 137045. [CrossRef]
30. Wan, F.; Zhong, G.; Wu, S.; Jiang, X.; Liao, J.; Zhang, X.; Zhang, H.; Mehmood, K.; Tang, Z.; Hu, L. Arsenic and antimony co-induced nephrotoxicity via autophagy and pyroptosis through ROS-mediated pathway in vivo and in vitro. *Ecotoxicol. Environ. Saf.* **2021**, *221*, 112442. [CrossRef]
31. Lewińska, K.; Karczewska, A. Antimony in soils of SW Poland—An overview of potentially enriched sites. *Environ. Monit. Assess.* **2019**, *191*, 70. [CrossRef] [PubMed]
32. Johnson, C.A. Antimony, a challenge for environmental scientists. In *The L.A. Colding Lecture Series in Environmental Science and Technology, Abstract*; Technical University of Denmark: Lyngby, Denmark, 2008.
33. Emsley, J. Nature's Building Blocks. In *An A–Z Guide to the Elements*; Oxford University Press: Oxford, UK, 2001.
34. Shotyk, W.; Krachler, M.; Chen, B. Anthropogenic impacts on the biogeochemistry and cycling of antimony. In *Metal Ions in Biological Systems 44 (Biogeochemistry, Availability and Transport of Metals in the Environment)*; Sigel, H., Sigel, R., Eds.; Marcel Dekker: Heidelberg, Germany, 2005; pp. 171–203, Chapter 7.
35. VROM. Circular on Target Values and Intervention Values for Soil Remediation. In *Dutch Ministry of Housing Spatial Planning and Environment (VROM)*; Annex, A., Ed.; VROM: The Hague, The Netherlands, 2000.
36. CCME. Canadian Soil Quality Guidelines for the Protection of Environmental and Human Health: Summary Table. In *Canadian Council of Ministers of the Environment*; CCME: Winnipeg, MB, Canada, 1999.
37. Arditsoglou, A.; Samara, C. Levels of total suspended particulate matter and major trace elements in Kosovo: A source identification and appointment study. *Chemosphere* **2005**, *59*, 669–678. [CrossRef] [PubMed]
38. Weckwerth, G. Verification of traffic emitted aerosol components in the ambient air of Cologne (Germany). *Atmos. Environ.* **2001**, *35*, 5525–5536. [CrossRef]

39. Gomez, D.; Fernanda Giné, M.; Claudia Sánchez Bellato, A.; Smichowski, P. Antimony: A traffic-related element in the atmosphere of Buenos Aires, Argentina. *J. Environ. Monit. JEM* **2005**, *7*, 1162–1168. [CrossRef]
40. Iijima, A.; Sato, K.; Fujitani, Y.; Fujimori, E.; Saito, Y.; Tanabe, K.; Ohara, T.; Kozawa, K.; Furuta, N. Clarification of the predominant emission sources of antimony in airborne particulate matter and estimation of their effects on the atmosphere in Japan. *Environ. Chem.* **2009**, *6*, 122–132. [CrossRef]
41. Földi, C.; Sauermann, S.; Dohrmann, R.; Mansfeldt, T. Traffic-related distribution of antimony in roadside soils. *Environ. Pollut.* **2018**, *237*, 704–712. [CrossRef]
42. Li, G.; Sun, G.; Ren, Y.; Luo, X.; Zhu, Y. Urban soil and human health: A review. *Eur. J. Soil Sci.* **2018**, *69*, 196–215. [CrossRef]
43. Jahandari, A.; Abbasnejad, A.; Jamasb, R. Concentration, likely sources, and ecological risk assessment of potentially toxic elements in urban soils of Shiraz City, SW Iran: A preliminary assessment. *Arab. J. Geosci.* **2020**, *13*, 936. [CrossRef]
44. Bineshpour, M.; Payandeh, K.; Nazarpour, A.; Sabzalipour, S. Status, source, human health risk assessment of potential toxic elements (PTEs), and Pb isotope characteristics in urban surface soil, case study: Arak city, Iran. *Environ. Geochem. Health* **2021**, *43*, 4939–4958. [CrossRef] [PubMed]
45. Sun, L.; Guo, D.; Liu, K.; Meng, H.; Zheng, Y.; Yuan, F.; Zhu, G. Levels, sources, and spatial distribution of heavy metals in soils from a typical coal industrial city of Tangshan, China. *Catena* **2019**, *175*, 101–109. [CrossRef]
46. Han, Q.; Wang, M.; Cao, J.; Gui, C.; Liu, Y.; He, X.; He, Y.; Liu, Y. Health risk assessment and bioaccessibilities of heavy metals for children in soil and dust from urban parks and schools of Jiaozuo, China. *Ecotoxicol. Environ. Saf.* **2020**, *191*, 110157. [CrossRef] [PubMed]
47. Morera-Gómez, Y.; Alonso-Hernández, C.; Armas-Camejo, A.; Viera-Ribot, O.; Morales, M.C.; Alejo, D.; Elustondo, D.; Lasheras, E.; Santamaría, J. Pollution monitoring in two urban areas of Cuba by using *Tillandsia recurvata* (L.) L. and top soil samples: Spatial distribution and sources. *Ecol. Indic.* **2021**, *126*, 107667. [CrossRef]
48. Pecina, V.; Brtnický, M.; Baltazár, T.; Juřička, D.; Kynický, J.; Galiová, M.V. Human health and ecological risk assessment of trace elements in urban soils of 101 cities in China: A meta-analysis. *Chemosphere* **2021**, *267*, 129215. [CrossRef] [PubMed]
49. Wu, D.; Yu, X.; Lai, M.; Feng, J.; Dong, X.; Peng, W.; Su, S.; Zhang, X.; Wan, L.; Jacobs, D.F.; et al. Diversified effects of co-planting landscape plants on heavy metals pollution remediation in urban soil amended with sewage sludge. *J. Hazard. Mater.* **2021**, *403*, 123855. [CrossRef]
50. Yuan, X.; Xue, N.; Han, Z. A meta-analysis of heavy metals pollution in farmland and urban soils in China over the past 20 years. *J. Environ. Sci.* **2021**, *101*, 217–226. [CrossRef]
51. Thestorf, K.; Makki, M. Pseudo-total antimony content in topsoils of the Berlin Metropolitan Area. *J. Soils Sediments* **2020**, *21*, 2102–2117. [CrossRef]
52. Tashakor, M.; Modabberi, S.; Argyraki, A. Assessing the contamination level, sources and risk of potentially toxic elements in urban soil and dust of Iranian cities using secondary data of published literature. *Environ. Geochem. Health* **2022**, *44*, 645–675. [CrossRef]
53. Soltani-Gerdefaramarzi, S.; Ghasemi, M.; Gheysouri, M. Pollution, human health risk assessment and spatial distribution of toxic metals in urban soil of Yazd City, Iran. *Environ. Geochem. Health* **2021**, *43*, 3469–3484. [CrossRef]
54. Vaziri, A.; Nazarpour, A.; Ghanavati, N.; Babainejad, T.; Watts, M.J. An integrated approach for spatial distribution of potentially toxic elements (Cu, Pb and Zn) in topsoil. *Sci. Rep.* **2021**, *11*, 7806. [CrossRef] [PubMed]
55. Dehghani, S.; Moore, F.; Keshavarzi, B.; Hale, B. Health risk implications of potentially toxic metals in street dust and surface soil of Tehran, Iran. *Ecotoxicol. Environ. Saf.* **2017**, *136*, 92–103. [CrossRef]
56. Piazzetta, K.D.; Ramsdorf, W.; Maranho, L. Use of airplant *Tillandsia recurvata* L.; Bromeliaceae, as biomonitor of urban air pollution. *Aerobiologia* **2018**, *35*, 125–137. [CrossRef]
57. Ashraf, M.A.; Maah, M.J.; Yusoff, I. Soil contamination, risk assessment and remediation. *Environ. Risk Sssessment Soil Contam.* **2014**, *1*, 3–56. [CrossRef]
58. Yousefi, M.; Ashrafi, A. Urban growth modeling in Bojnurd by using remote sensing data (Based on neural network and Markov modeling changes). *J. Reg. Plan.* **2016**, *6*, 179–192. (In Persian)
59. Orgiazzi, A.; Ballabio, C.; Panagos, P.; Jones, A.; Fern'andez-Ugalde, O. LUCAS Soil, the largest expandable soil dataset for Europe: A review. *Eur. J. Soil Sci.* **2018**, *69*, 140–153. [CrossRef]
60. IAEA (International Atomic Energy Agency). *Soil Sampling for Environmental Contaminants*; IAEATECDOC-1415; IAEA: Vienna, Austria, 2004.
61. Man, Y.B.; Sun, X.L.; Zhao, Y.G.; Lopez, B.N.; Chung, S.S.; Wu, S.C.; Cheung, K.C.; Wong, M.H. Health risk assessment of abandoned agricultural soils based on heavy metal contents in Hong Kong, the world's most populated city. *Environ. Int.* **2010**, *36*, 570–576. [CrossRef]
62. Tanner, P.A.; Ma, H.L.; Yu, P.K. Fingerprinting metals in urban street dust of Beijing, Shanghai, and Hong Kong. *Environ. Sci. Technol.* **2008**, *42*, 7111–7117. [CrossRef] [PubMed]
63. USEPA. *Exposure Factors Handbook, Volume 1: General Factors*; U.S. Environmental Protection Agency, Office of Research and Development: Washington, DC, USA, 1997.
64. Soltani, N.; Keshavarzi, B.; Moore, F.; Tavakol, T.; Lahijanzadeh, A.R.; Jaafarzadeh, N.; Kermani, M. Ecological and human health hazards of heavy metals and polycyclic aromatic hydrocarbons (PAHs) in road dust of Isfahan metropolis, Iran. *Sci. Total Environ.* **2015**, *505*, 712–723. [CrossRef]

65. Chen, H.; Teng, Y.; Lu, S.; Wang, Y.; Wang, J. Contamination features and health risk of soil heavy metals in China. *Sci. Total Environ.* **2015**, *512*, 143–153. [CrossRef]
66. Ryan, J.; Estefan, G.; Rashid, A. *Soil and Plant Analysis Laboratory Manual*; ICARDA: Beirut, Lebanon, 2001.
67. Rouhani, A.; Bradák, B.; Makki, M.; Ashtiani, B.; Hejcman, M. Ecological risk assessment and human health risk exposure of heavy metal pollution in the soil around an open landfill site in a developing country (Khesht, Iran). *Arab. J. Geosci.* **2022**, *15*, 1523. [CrossRef]
68. Muller, G. Schwermetalle in den Sedimenten des Rheins-Veränderungen seit 1971. *Umschau* **1969**, *79*, 778–783.
69. Håkanson, L. An ecological risk index for aquatic pollution control. A sedimentological approach. *Water Res.* **1980**, *14*, 975–1001. [CrossRef]
70. Rouhani, A.; Shahivand, R. Potential ecological risk assessment of heavy metals in archaeology on an example of the Tappe Rivi (Iran). *SN Appl. Sci.* **2020**, *2*, 1–11. [CrossRef]
71. USEPA. *Risk Assessment Guidance for Superfund. Volume I. Human Health Evaluation Manual (Part A)*; EPA/540/1-89/002; US Environmental Protection Agency: Washington, DC, USA, 1989.
72. Rouhani, A.; Azimzadeh, H.; Sotoudeh, A.; Ehdaei, A. Health Risk Assessment of Heavy Metals in Archaeological Soils of Tappe Rivi Impacted by Ancient Anthropogenic Activity. *Chem. Africa* **2022**, *5*, 1751–1764. [CrossRef]
73. USEPA. *Risk Assessment Guidance for Superfund: Volume III—Part A, Process for Conducting Probabilistic Risk Assessment*; EPA 540-R-02-002; US Environmental Protection Agency: Washington, DC, USA, 2001.
74. USEPA. Regional Screening Levels (RSLs)—Generic Tables (May 2016). 2016. Available online: https://19january2017snapshot.epa.gov/risk/regional-screening-levels-rsls-generic-tables-may-2016_.html (accessed on 25 May 2020).
75. Pan, L.; Wang, Y.Y.; Ma, J.; Hu, Y.; Su, B.; Fang, G.; Wang, L.; Xiang, B. A review of heavy metal pollution levels and health risk assessment of urban soils in Chinese cities. *Environ. Sci. Pollut. Res.* **2017**, *25*, 1055–1069. [CrossRef]
76. Kusin, F.M.; Azani, N.F.; Hasan, S.N.; Sulong, N.A. Distribution of heavy metals and metalloid in surface sediments of heavily-mined area for bauxite ore in Pengerang, Malaysia and associated risk assessment. *Catena* **2018**, *165*, 454–464. [CrossRef]
77. Konstantinova, E.; Minkina, T.M.; Sushkova, S.; Konstantinov, A.O.; Rajput, V.D.; Sherstnev, A.K. Urban soil geochemistry of an intensively developing Siberian city: A case study of Tyumen, Russia. *J. Environ. Manag.* **2019**, *239*, 366–375. [CrossRef]
78. Utermann, J.; Fuchs, M.; Düwel, O. *Flächenrepräsentative Hintergrundwerte für Arsen, Antimon, Beryllium, Molybdän, Kobalt, Selen, Thallium, Uran und Vanadium in Böden Deutschlands aus länderübergreifender Sicht*; Bundesanstalt für Geowissenschaften und Rohstoffe: Hannover, Germany, 2008.
79. Wang, H.; Lu, S. Spatial distribution, source identification and affecting factors of heavy metals contamination in urban–suburban soils of Lishui city, China. *Environ. Earth Sci.* **2011**, *64*, 1921–1929. [CrossRef]
80. Yan, G.; Mao, L.; Liu, S.; Mao, Y.; Ye, H.; Huang, T.; Li, F.; Chen, L. Enrichment and sources of trace metals in roadside soils in Shanghai, China: A case study of two urban/rural roads. *Sci. Total Environ.* **2018**, *631–632*, 942–950. [CrossRef]
81. Kabata-Pendias, A. *Trace Elements in Soils and Plants*, 3rd ed.; CRC Press: Boca Raton, FL, USA, 2000.
82. Okoye, E.A.; Ezejiofor, A.N.; Nwaogazie, I.L.; Frazzoli, C.; Orisakwe, O.E. Heavy Metals and Arsenic in Soil and Vegetation of Niger Delta, Nigeria: Ecological Risk Assessment. Case Stud. *Chem. Environ. Eng* **2022**, *6*, 100222. [CrossRef]
83. Reimann, C.; Fabian, K. Quantifying diffuse contamination: Comparing silver and mercury in organogenic and minerogenic soil. *Sci. Total Environ.* **2022**, *832*, 155065. [CrossRef]
84. Zhang, D.; Lee, D.J.; Pan, X. Potentially harmful metals and metalloids in urban street dusts of Urumqi City: Comparison with Taipei City. *J. Taiwan Instit. Chem. Eng.* **2014**, *45*, 2447–2450. [CrossRef]
85. Hjortenkrans, D.S.; Bergbäck, B.G.; Häggerud, A.V. New Metal Emission Patterns in Road Traffic Environments. *Environ. Monit. Assess.* **2006**, *117*, 85–98. [CrossRef] [PubMed]
86. von Uexküll, O.; Skerfving, S.; Doyle, R.; Braungart, M. Antimony in brake pads—A carcinogenic component? *J. Clean. Prod.* **2005**, *13*, 19–31. [CrossRef]
87. Iijima, A.; Sato, K.; Yano, K.; Kato, M.; Kozawa, K.; Furuta, N. Emission factor for antimony in brake abrasion dusts as one of the major atmospheric antimony sources. *Environ. Sci. Technol.* **2008**, *42*, 2937–2942. [CrossRef] [PubMed]
88. Duong, T.T.; Lee, B. Determining contamination level of heavy metals in road dust from busy traffic areas with different characteristics. *J. Environ. Manag.* **2011**, *92*, 554–562. [CrossRef]
89. Sezgin, N.; Ozcan, H.K.; Demir, G.; Nemlioglu, S.; Bayat, C. Determination of heavy metal concentrations in street dusts in Istanbul E-5 highway. *Environ. Int.* **2004**, *29*, 979–985. [CrossRef]
90. Al-Khashman, O.A. Determination of metal accumulation in deposited street dusts in Amman. *Jordan Environ. Geochem. Health* **2007**, *29*, 1–10. [CrossRef]
91. Raghunath, R.; Tripathi, R.M.; Kumar, A.; Sathe, A.P.; Khandekar, R.N.; Nambi, K.S. Assessment of Pb, Cd, Cu, and Zn exposures of 6- to 10-year-old children in Mumbai. *Environ. Res.* **1999**, *80*, 215–221. [CrossRef]
92. Guney, M.; Onay, T.T.; Copty, N.K. Impact of overland traffic on heavy metal levels in highway dust and soils of Istanbul, Turkey. *Environ. Monit. Assess.* **2010**, *164*, 101–110. [CrossRef]
93. CEPA. *Canadian Soil Quality Guidelines for the Protection of Environmental and Human Health*; CEPA: Washington, DC, USA, 2007.
94. Yabe, J.; Ishizuka, M.; Umemura, T. Current levels of heavy metal pollution in Africa. *J. Vet. Med. Sci.* **2010**, *72*, 1257–1263. [CrossRef]

95. Simon, E.; Vidic, A.; Braun, M.; Fábián, I.; Tóthmérész, B. Trace element concentrations in soils along urbanization gradients in the city of Wien, Austria. *Environ. Sci. Pollut. Res.* **2012**, *20*, 917–924. [CrossRef]
96. Imperato, M.; Adamo, P.; Naimo, D.; Arienzo, M.M.; Stanzione, D.; Violante, P. Spatial distribution of heavy metals in urban soils of Naples city (Italy). *Environ. Pollut.* **2003**, *124*, 247–256. [CrossRef] [PubMed]
97. Wei, B.; Yang, L. A review of heavy metal contaminations in urban soils, urban road dusts and agricultural soils from China. *Microchem. J.* **2010**, *94*, 99–107. [CrossRef]
98. Luo, X.; Ding, J.; Xu, B.; Wang, Y.; Li, H.; Yu, S. Incorporating bioaccessibility into human health risk assessments of heavy metals in urban park soils. *Sci. Total Environ.* **2011**, *424*, 88–96. [CrossRef] [PubMed]
99. Li, S.; Yang, L.; Chen, L.; Zhao, F.; Sun, L. Spatial distribution of heavy metal concentrations in peri-urban soils in eastern China. *Environ. Sci. Pollut. Res.* **2018**, *26*, 1615–1627. [CrossRef]
100. Wang, J.; Li, S.; Cui, X.; Li, H.; Qian, X.; Wang, C.; Sun, Y. Bioaccessibility, sources and health risk assessment of trace metals in urban park dust in nanjing, southeast China. *Ecotoxicol. Environ. Saf.* **2016**, *128*, 161–170. [CrossRef] [PubMed]
101. Said, I.; Salman, S.A.E.-R.; Samy, Y.; Awad, S.A.; Melegy, A.; Hursthouse, A.S. Environmental factors controlling potentially toxic element behaviour in urban soils, El Tebbin, Egypt. *Environ. Monit. Assess.* **2019**, *191*, 267. [CrossRef]
102. Pobi, K.K.; Nayek, S.; Gope, M.; Rai, A.K.; Saha, R. Sources Evaluation, Ecological and Health Risk Assessment of Potential Toxic Metals (PTMs) in Surface Soils of an Industrial Area. *Environ. Geochem. Health India* **2020**, *42*, 4159–4180. [CrossRef]
103. Fei, X.; Christakos, G.; Lou, Z.; Xiao, R.; Lv, X.; Ren, Z. Assessment and source apportionment of toxic metal in soils using integrated positive matrix factorization and Bayesian maximum entropy: A case study in Z county, southeastern China. *Ecol. Indic.* **2022**, *145*, 109647. [CrossRef]
104. Shrivastava, A.; Barla, A.; Majumdar, A.; Singh, S.; Bose, S. Arsenic mitigation in rice grain loading via alternative irrigation by proposed water management practices. *Chemosphere* **2020**, *238*, 124988. [CrossRef]
105. Majumdar, A.; Upadhyay, M.K.; Ojha, M.; Afsal, F.; Giri, B.; Srivastava, S.; Bose, S. Enhanced phytoremediation of Metal (loid) s via spiked ZVI nanoparticles: An urban clean-up strategy with ornamental plants. *Chemosphere* **2022**, *288*, 132588. [CrossRef]
106. Zhang, B.; Jia, T.; Peng, S.; Yu, X.; She, D. Spatial distribution, source identification, and risk assessment of heavy metals in the cultivated soil of the Qinghai–Tibet Plateau region: Case study on Huzhu County. *Glob. Ecol. Conserv.* **2022**, *35*, e02073. [CrossRef]
107. Jadoon, S.; Muhammad, S.; Hilal, Z.; Ali, M.J.; Khan, S.; Khattak, N.U. Spatial distribution of potentially toxic elements in urban soils of Abbottabad city, (N Pakistan): Evaluation for potential risk. *Microchem. J.* **2020**, *153*, 104489. [CrossRef]
108. Chen, H.; Teng, Y.; Lu, S.; Wang, Y.; Wu, J.; Wang, J. Source apportionment and health risk assessment of trace metals in surface soils of Beijing metropolitan, China. *Chemosphere* **2016**, *144*, 1002–1011. [CrossRef] [PubMed]
109. Tyagi, N.; Upadhyay, M.K.; Majumdar, A.; Pathak, S.K.; Giri, B.; Jaiswal, M.K.; Srivastava, S. An assessment of various potentially toxic elements and associated health risks in agricultural soil along the middle Gangetic basin, India. *Chemosphere* **2022**, *300*, 134433. [CrossRef]
110. Li, F.; Yang, H.; Ayyamperumal, R.; Liu, Y. Pollution, sources, and human health risk assessment of heavy metals in urban areas around industrialization and urbanization-Northwest China. *Chemosphere* **2022**, *308*, 136396. [CrossRef] [PubMed]
111. Huang, Y.; Zhang, S.; Chen, Y.; Wang, L.; Long, Z.; Hughes, S.S.; Ni, S.; Cheng, X.; Wang, J.; Li, T.; et al. Tracing Pb and Possible Correlated Cd Contamination in Soils by Using Lead Isotopic Compositions. *J. Hazard. Mater.* **2019**, *385*, 121528. [CrossRef] [PubMed]
112. Wu, W.; Wu, P.; Yang, F.; Sun, D.; Zhang, D.X.; Zhou, Y.K. Assessment of heavy metal pollution and human health risks in urban soils around an electronics manufacturing facility. *Sci. Total Environ.* **2018**, *630*, 53–61. [CrossRef] [PubMed]
113. Ghani, J.; Nawab, J.; Faiq, M.E.; Ullah, S.; Alam, A.; Ahmad, I.; Ali, S.W.; Khan, S.; Ahmad, I.; Muhammad, A.; et al. Multi-geostatistical analyses of the spatial distribution and source apportionment of potentially toxic elements in urban children's park soils in Pakistan: A risk assessment study. *Environ. Pollut.* **2022**, *311*, 119961. [CrossRef]
114. Shen, W.; Hu, Y.; Zhang, J.; Zhao, F.; Bian, P.; Liu, Y. Spatial distribution and human health risk assessment of soil heavy metals based on sequential Gaussian simulation and positive matrix factorization model: A case study in irrigation area of the Yellow River. *Ecotoxicol. Environ. Saf.* **2021**, *225*, 112752. [CrossRef]
115. Ghanavati, N.; Nazarpour, A.; De Vivo, B. Ecological and human health risk assessment of toxic metals in street dusts and surface soils in Ahvaz Iran. *Environ. Geochem. Health* **2019**, *41*, 875–891. [CrossRef]
116. Ihedioha, J.; Ukoha, P.; Ekere, N. Ecological and human health risk assessment of heavy metal contamination in soil of a municipal solid waste dump in Uyo Nigeria. *Environ. Geochem. Health* **2017**, *39*, 497–515. [CrossRef] [PubMed]
117. Tongo, I.; Ogbeide, O.; Ezemonye, L. Human health risk assessment of polycyclic aromatic hydrocarbons (PAHs) in smoked fish species from markets in Southern Nigeria. *Toxicol. Rep.* **2017**, *4*, 55–61. [CrossRef] [PubMed]
118. De Miguel, E.; Iribarren, I.; Chacón, E.; Ordóñez, A.; Charlesworth, S. Risk-based evaluation of the exposure of children to trace elements in playgrounds in Madrid (Spain). *Chemosphere* **2007**, *66*, 505–513. [CrossRef]
119. Cao, S.; Duan, X.; Zhao, X.; Wang, B.; Ma, J.; Fan, D.; Sun, C.; He, B.; Wei, F.; Jiang, G. Health risk assessment of various metal(loid)s via multiple exposure pathways on children living near a typical lead-acid battery plant, China. *Environ. Pollut.* **2015**, *200*, 16–23. [CrossRef]
120. Cheng, Z.; Chen, L.; Li, H.; Lin, J.; Yang, Z.; Yang, Y.; Xu, X.; Xian, J.; Shao, J.; Zhu, X. Characteristics and health risk assessment of heavy metals exposure via household dust from urban area in Chengdu, China. *Sci. Total Environ.* **2018**, *619–620*, 621–629. [CrossRef] [PubMed]

121. Jiang, Y.; Chao, S.; Liu, J.; Yang, Y.; Chen, Y.; Zhang, A.; Cao, H. Source apportionment and health risk assessment of heavy metals in soil for a township in Jiangsu Province, China. *Chemosphere* **2017**, *168*, 1658–1668. [CrossRef]
122. Timofeev, I.V.; Kosheleva, N.E.; Kasimov, N.S. Health risk assessment based on the contents of potentially toxic elements in urban soils of Darkhan, Mongolia. *J. Environ. Manag.* **2019**, *242*, 279–289. [CrossRef] [PubMed]
123. USEPA. *Supplemental Guidance for Developing Soil Screening Levels for Superfund Sites*; US Environmental Protection Agency: Washington, DC, USA, 2001.
124. USEPA. *Supplemental Guidance for Developing Soil Screening Levels for Superfund Sites*; US Environmental Protection Agency: Washington, DC, USA, 2002; Volume 106.
125. USEPA. *Integrated Risk Information System of the US Environmental Protection Agency*; US Environmental Protection Agency: Washington, DC, USA, 2012.
126. USEPA. *Regional Screening Level (RSL) Resident Soil Table (TR=1E-06, HQ=1) May 718 2020 (Corrected)*; US Environmental Protection Agency: Washington, DC, USA, 2020. Available online: https://support.esdat.net/Environmental%20Standards/us/region_3_6_9/regional%20screening%20level%20(rsl)%20summary%20table%20(tr=1e-06,%20hq=1)%20may%202020%20(corrected).pdf (accessed on 9 October 2020).